Available online at www.sciencedirect.com

SCIENCE DIRECT®

Developmental Biology 266 (2004) 161–177

DEVELOPMENTAL BIOLOGY

www.elsevier.com/locate/ydbio

Murine numb regulates granule cell maturation in the cerebellum

Anne-Laurence Klein,[a,b,1] Olav Zilian,[c,1] Ueli Suter,[b] and Verdon Taylor[a,*]

[a] *Max Planck Institute of Immunobiology, Department of Molecular Embryology, Stubeweg 51, D-79108 Freiburg, Germany*
[b] *Institute of Cell Biology, Department of Biology, Swiss Federal Institute of Technology, ETH-Honggerberg, CH-8093 Zurich, Switzerland*
[c] *Swiss Institute of Experimental Cancer Research, CH-1066 Epalinges, Switzerland*

Received for publication 13 August 2003, revised 6 October 2003, accepted 15 October 2003

Abstract

Notch is a key regulator of vertebrate neurogenesis and the cytoplasmic adaptor protein Numb is a modulator of the Notch signaling pathway. To address the role of murine Numb in development of the central nervous system, we used a conditional gene ablation approach. We show that Numb is involved in the maturation of cerebellar granule cells. Although the specification of neural cell fates in the cerebellum is not affected in the absence of Numb, the transition from a mitotic progenitor to a mature granule cell is aberrant and migration of postmitotic granule cells to the internal granule cell layer is delayed. In some animals, this results in a complete agenesis of granule cells and a strong ataxia. We confirmed these findings in vitro and found that *Numb*-deficient cerebellar progenitor cells show a marked delay in granule cell maturation. Our results suggest that Numb plays a role in the transition of a mitotic progenitor to a fully differentiated granule cell in the cerebellum. In addition, the maturation of Purkinje cells is also delayed in *Numb*-deficient mice.

Keywords: Numb; Notch; Neurogenesis; CNS; Cerebellum; Granule cells

Introduction

Cells of the vertebrate nervous system are generated from the neuroepithelium during embryonic development. A subpopulation of cells within the neuroepithelium displays stem cell-like properties: multipotency, the capacity for self-renewal and the ability to generate other cell-types through asymmetric cell division. The differentiation of these neural stem cells likely involves a precursor-like state before generation of the multiple cell-types of the brain (Mayer-Proschel et al., 1997; Rao and Mayer-Proschel, 1997). Neural precursor cells acquire a defined identity from their axial coordinates within the neuroepithelium. Thus, the development of stem cells into the various differentiated neural cell types of the adult nervous system must be strictly coordinated in a temporal and spatial manner. The mechanisms that control the development of the vertebrate nervous system are only partially known. In *Drosophila*, Delta-Notch signaling regulates neurogenesis through lateral inhibition (Heitzler and Simpson, 1991; Muskavitch, 1994). However, cell-intrinsic mechanisms also play a role in the development of the *Drosophila* nervous system. *Drosophila* Numb (dNumb) has been found to be an important regulator of asymmetric cell division and fate determination in the nervous system, muscle and malpighian tubules of *Drosophila* (Frise et al., 1996; Guo et al., 1996; Spana and Doe, 1996; Wan et al., 2000). Genetic analyses have indicated that dNumb is involved in Notch signaling and that the two genes have reciprocal functions (Rhyu et al., 1994; Wang et al., 1997). Furthermore, dNumb/Notch signaling has been shown to regulate the choice between neuronal cell fate or programmed cell death (Lundell et al., 2003). Numb is a cytoplasmic, membrane-associated protein with an N-terminal phosphotyrosine-binding (PTB) domain, a proline-rich region (PRR) and an EH-binding site at the C-terminus (Dho et al., 1998; Mayer, 1999; Salcini et al., 1997). Numb has been claimed to bind to the intracellular domain (ICD) of Notch via its PTB domain in a phosphotyrosine-independent manner to prevent Notch signaling through an as yet unclear mechanism (Wakamatsu et al., 1999; Zhong et al., 1997). However, recent data suggest that dNumb regulates Notch activity by affecting the subcellular localization of the

* Corresponding author. Max Planck Institute of Immunobiology, Department of Molecular Embryology, Stubeweg 51, D-79108 Freiburg, Germany. Fax: +49-761-5108-474.
E-mail address: taylor@immunbio.mpg.de (V. Taylor).
[1] These authors contributed equally to the work.

0012-1606/$ - see front matter © 2003 Elsevier Inc. All rights reserved.
doi:10.1016/j.ydbio.2003.10.017

tetraspan protein *sanpodo* (O'Connor-Giles et al., 2003), and that mammalian Numb is involved in Notch1 receptor ubiquitination and proteasomal degradation but may not interact directly with Notch1 (McGill and McGlade, 2003).

During vertebrate central nervous system (CNS) development, neuroepithelial cells proliferate in the ventricular zone to enlarge the stem cell pool (Chenn and McConnell, 1995). Subsequently, stem cell progeny delaminate from the ventricular surface and start to differentiate. In the developing chick CNS, chicken Numb (cNumb) protein is reported to be localized to the basal pole of neuroepithelial cells during M-phase of the cell cycle (Silva et al., 2002; Wakamatsu et al., 1999). Symmetric cell division results in the formation of two identical daughter cells that acquire Numb. During asymmetric cell division, cNumb is preferentially inherited by the basal daughter cell that differentiates, leaving the apical cNumb-depleted daughter cell as a progenitor. Retroviral overexpression of Numb in the chick neuroepithelium resulted in exit from the cell cycle and precocious neuronal differentiation. By contrast, retroviral overexpression of Notch1 ICD in the neuroepithelium resulted in an enlargement of the stem cell pool and a delay in neurogenesis (Wakamatsu et al., 1999). These results suggest that in the chicken, cNumb is prominently involved as a cell-intrinsic cue in early developmental decisions made by neural progenitor cells. However, in mammals, the situation is less clear. In vitro overexpression of mammalian mNumb in the neural crest-derived MONC-1 cell line leads to the generation of neurons at the expense of glia and smooth muscle cells and a bias in P19 cell differentiation into neurons instead of glia (Verdi et al., 1996, 1999). In addition, isoforms of human Numb (hNumb) generated by alternative RNA splicing with a long PRR rather promote proliferation while hNumb isoforms with a short PRR promote differentiation of P19 cells (Verdi et al., 1996, 1999).

Between E8.5 and E12.5, expression of Numb (mNumb) overlaps with that of Notch1 expression in neuroepithelial cells of the ventricular zone and it is localized to the apical pole of mitotic cells (Zhong et al., 1996, 1997). In cortical progenitors and neuroblasts, asymmetric localization of mNumb during cell division affects the fate acquired by the daughter cells (Shen et al., 2002). Furthermore, asymmetric distribution of Numb is also seen in the rat retinal neuroepithelium (Cayouette and Raff, 2002). Asymmetric distribution of Numb and the dynamic expression of different Numb isoforms at specific time points during rat retinal development are associated with the temporally controlled generation of the different retinal cell types (Dooley et al., 2003).

Two independent *mNumb*-deficient mouse lines have been generated that show severe cranial neural tube closure defects and die around embryonic day 11.5 (E11.5), possibly as a result of vasculature malformations (Zhong et al., 2000; Zilian et al., 2001). The in vivo role of mNumb in mammalian neurogenesis and the fate of *Numb*-deficient neuroepithelial cells remain unclear due to the early lethality of *Numb*-deficient mice (Zhong, 2003; Zhong et al., 2000; Zilian et al., 2001). To address the function of mNumb during vertebrate CNS development, we have conditionally ablated the *mNumb* gene from the mouse neural tube using the Cre-*lox* system. Numb was inactivated specifically in neuroepithelial cells of the midbrain–hindbrain boundary by expression of Cre-recombinase from an *engrailed2* promoter to circumvent the lethal effects of mNumb loss-of-function. We followed the consequences of *mNumb* ablation on neuroepithelial cells and their progeny through to adulthood and found that mNumb is involved in the transition of cerebellar progenitors to mature granule cells.

Materials and methods

Generation of mice and breeding

Mice carrying *loxP*-flanked *Numb* alleles have been described previously (Zilian et al., 2001) and mice carrying the cre-recombinase under the transcriptional control of the *engrailed-2* promoter enhancer (line Tg3) were kindly provided by Dr. A. Joyner (Zinyk et al., 1998). The ROSA26-R Cre-reporter (*R26R*) transgenic line was provided by Dr. P. Soriano (1999). Embryos were generated by timed-mating, counting the morning after pairing as embryonic day 0.5. The animals were maintained on a mixed 129SV/C57BL6 background and sacrificed according to institutional guidelines.

In situ hybridization analysis of gene expression

Embryos and brains were isolated and frozen in OCT (TissueTech) on dry ice. Frozen sections (20 μm) were thaw-mounted onto Superfrost slides (Mettler), air-dried and fixed in 4% paraformaldehyde. The midline sagittal sections of the adult cerebellum were orientated between the peduncles. The embryos were mounted and cross-sections cut perpendicular to the neural tube at the level of the isthmic flexure. In situ RNA hybridization was performed with digoxigenin-labeled RNA probes for calbindin D28k, Mash1, Math1 (Atoh1-Mouse Genome Informatics) and NeuroD, as described previously (Lutolf et al., 2002).

Immunohistochemistry and cell fate analysis

Histological analysis was performed by staining paraffin sections (5 μm) for 2 min in hematoxylin (Polysciences, Inc.) and 10 min in eosin (Polysciences, Inc.) followed by dehydration in alcohol and embedding in DePex (Serva). Indirect immunofluorescence was performed on frozen sections (20 μm) with antibodies against Nestin (monoclonal mouse antibody, 1:30; R401, Developmental Studies Hybridoma Bank, University of Iowa) and phosphohistone H3 (pH3) (polyclonal rabbit antibody, 1:300; Upstate Bio-

technology). Sections were fixed in 4% paraformaldehyde and blocked in PBS 0.2% Tween20 containing 5% goat serum (blocking buffer). Antibodies were diluted in blocking buffer and incubated overnight at 4°C. Immunostaining against Calbindin D28k (monoclonal mouse antibody, 1:200; Sigma) and GABAα6 (polyclonal rabbit antibody, 1:1000; Chemicon) was performed on paraffin sections (5 μm) using standard protocols. Bound antibody was detected with Cy3- or FITC-conjugated goat anti-mouse Ig (Jackson Labs) and goat anti-rabbit Ig (Jackson Labs). Bound GABAα6 receptor subunit antibody was visualized colorimetrically with HRP-conjugated anti-rabbit Ig using the DAKO Envision™ + HRP system (DAKO) according to the manufacturer's instructions. β-galactosidase was detected by X-gal staining according to Zinyk et al. (1998) or with anti-β-galactosidase antibodies (polyclonal rabbit antibody, 1:100; Cappel). Apoptotic cell death was detected by TUNEL staining using biotin-labeled UTP and a Cy3-conjugated streptavidin complex according to the manufacturer's instructions (Roche Diagnostics). Images were collected using an Axiophot microscope (Zeiss) in conjunction with a ProgRes 3008 (Jenoptik) or Hamamatsu (Hamamatsu Photonics) CCD camera; image processing was performed with NIH Image and Adobe Photoshop 7.0 software.

Isolation and culture of cerebellar neuroepithelial cells and immunocytochemistry

Embryonic day 10.5 embryos were sacrificed and the cerebellar primordium dissected under sterile conditions (Fig. 9A). The trunk region of the embryos was used for DNA isolation and genotyping by PCR. The cerebellar primordium of the individual embryos was dissociated and incubated in Dulbecco's Modified Eagle Medium/F12 (DMEM/F12; Life Technologies) containing 1 mg/ml collagenase type IV (Sigma), 0.12 mg/ml hyaluronidase (Sigma) and 0.03 mg/ml trypsin inhibitor (Sigma) for 10 min at 37°C. The cells were collected by centrifugation and resuspended in differentiation medium consisting of DMEM/F12 containing 1% N2 (Gibco), 25 mM KCL, 10 ng/ml EGF (Peprotech), 10 ng/ml FGF-2 (Peprotech), 5 ng/ml NGF (Peprotech), 10 ng/ml BDNF (Peprotech) and 10 ng/ml IGF1 (Peprotech). The cells from the cerebellar primordium of one embryo were plated on 8 wells (18 mm) of a 24-well plate coated with 50 μg/ml poly-L-lysine and 20 mg/ml laminin. No obvious differences in the plating efficiency were observed between mutant and control cells. The cells were cultured for 6.5 or 13 days in differentiation medium, and half of the medium was replaced every second day with medium containing double concentration of growth factors. The cells were fixed in 4% formaldehyde and immunostained with antibodies against β-TubulinIII (Tuj1) (monoclonal mouse antibody, 1:200; Sigma), Nestin (1:30; R401, Developmental Studies Hybridoma Bank), Calbindin D28k (monoclonal mouse antibody, 1:200; Sigma), smooth muscle actin (SMA) (monoclonal mouse antibody, 1:500; Sigma) and O4 (monoclonal mouse antibody, 1:10; a kind gift of Dr. M. Schwab) in conjunction with anti-β-galactosidase antibodies (polyclonal rabbit antibody, 1:100; Cappel). Additionally, cells were immunostained with antibodies against Math1 (polyclonal rabbit antibody, 1:200; a kind gift of Dr. J. Johnson). Bound antibody was detected with Cy3-conjugated goat anti-mouse Ig (Jackson Labs), FITC-goat anti-mouse IgM (Jackson Labs) or goat anti-rabbit Ig (Jackson Labs).

Western blot analysis

E12.5 embryos were sacrificed, the cerebellar primordium dissociated and the isolated cerebellar neuroepithelial cells of individual embryos were plated on sister plates in differentiation medium (see section above). After 5 days, half of the cells of each embryo were fixed and stained with anti-β-galactosidase antibodies to determine the percentage of recombined cells. The other half of the cells was washed and protein extracted in 8 M Urea. Twenty micrograms of protein of both control and mutant embryos were resolved on denaturing SDS-polyacrylamide gels. PonceauS staining was used to assess equal loading of proteins. The blots were incubated with a polyclonal rabbit anti-Numb antibody (1:800; kindly provided by Dr. H. Okano) at 4 °C overnight and detected by ECL (Amersham) chemiluminescence. The blot was stripped and incubated with an anti-βactin antibody (monoclonal mouse antibody, 1:1000; Sigma) for normalization. Quantification was performed using 1D Image Analysis Software (Kodak Digital Science).

Results

We have conditionally inactivated the *Numb* gene in neuroepithelial cells of the isthmus and cerebellar primordium at E9 using a Cre-*loxP* approach to circumvent the early embryonic lethality observed in Numb-deficient animals (Zhong et al., 2000; Zilian et al., 2001). Floxed *Numb* alleles were generated by introducing *loxP* sequences flanking the first coding exon of *mNumb* by homologous recombination (Fig. 1; Zilian et al., 2001). Cre-mediated recombination results in a null allele (Zilian et al., 2001). We restricted *mNumb* ablation to the midbrain–hindbrain region of the neural tube by expression of Cre-recombinase under the transcriptional control of the *engrailed2*-promoter enhancer (*En2-Cre*) (Fig. 1). Mice homozygous for the floxed *Numb* allele show no detectable abnormal phenotype in the absence of Cre-recombinase. In addition, the ROSA26 Cre-reporter allele (*R26R*) was included in the analysis to follow the recombination and fate of Cre-expressing cells and their progeny (Lutolf et al., 2002; Soriano, 1999). If Cre-recombinase is present, the *loxP* sequences flanking the PGK neo cassette of the *R26R* are

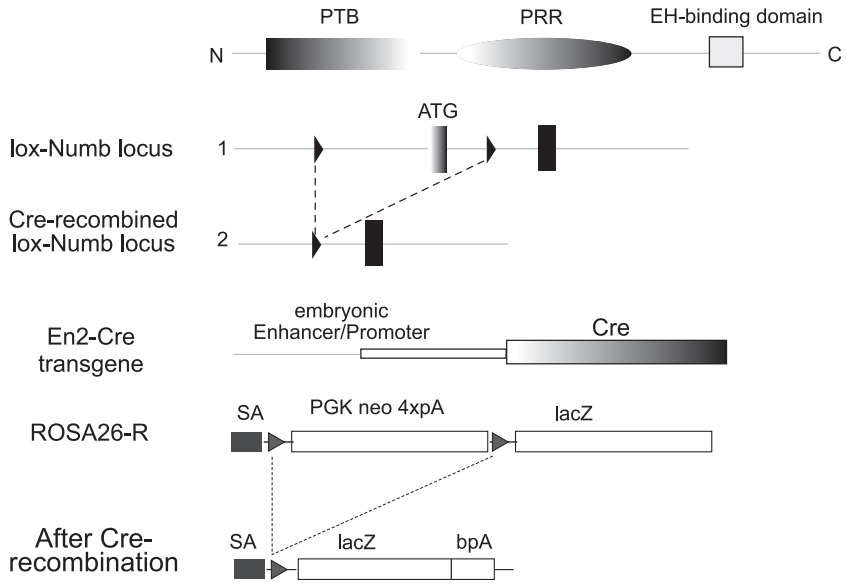

Fig. 1. Schematic structure of the *mNumb* and ROSA26-reporter conditional alleles. The exon encoding for the translation initiation sequence and the first 42 amino acids of the *mNumb* gene were flanked by loxP sequences (triangles) to generate the floxed *Numb* allele (1) and the null allele generated after Cre-induced recombination (2). Cre-recombinase was expressed from the Engrailed2 promoter enhancer sequences (*En2-Cre*) (Zinyk et al., 1998). The ROSA26-R Cre-reporter allele (*R26R*) was used to follow the fate of recombined cells (see Soriano, 1999 for details). Cre-mediated recombination deletes the PGK neo cassette and results in constitutive expression of β-galactosidase.

recombined and β-galactosidase is constitutively expressed (Soriano, 1999).

Conditional disruption of mNumb does not affect midbrain–hindbrain formation between E10.5 and E15

The ablation of *mNumb* in the CNS was restricted to the midbrain–hindbrain neuroepithelium by using the *En2-Cre* Tg3 transgenic line (Zinyk et al., 1998). Cre-mediated recombination was detected at E10.5 by X-gal staining in the midbrain–hindbrain neuroepithelium and in a restricted population of cells along the neural tube (Figs. 2A, B). Animals carrying heterozygous and homozygous floxed *Numb* alleles and an *En2-Cre* transgene showed a similar pattern of recombination at E10.5 (Fig. 2A). To elucidate whether conditional *Numb* ablation leads to changes in cell lineage determination and specification or differentiation, we analyzed the expression of the proneural genes *Mash1* and *Math1* at E12.5 by in situ hybridization. Mash1 is expressed by putative Purkinje cell precursors starting in the lateral cerebellar primordium at around E12.5 (Guillemot and Joyner, 1993). Both control and mutant embryos showed a similar pattern of Mash1 expression with no aberrant distribution at E12.5 (Figs. 2E, F), in contrast to findings made following conditional ablation of *Notch1* from the same region of the neural tube (Lutolf et al., 2002). Math1 is a proneural bHLH transcription factor required for cerebellar granule cell specification and differentiation and the earliest known marker for granule cell precursors (Ben-Arie et al., 1997). Again and in contrast to the effects of *Notch1* ablation, Math1 was detected in cells at the posterior edge of the cerebellar primordium forming the rhombic lip (Figs. 2C, D). As Notch signaling has been proposed to regulate the onset of neuroepithelial cell differentiation in vivo (de la Pompa, 1997; Lutolf et al., 2002) and Numb may also regulate progenitor cell differentiation (Petersen et al., 2002), we analyzed the expression of Nestin, an intermediate filament protein in undifferentiated cells. Immunostaining with Nestin-specific antibodies did not reveal obvious changes in progenitor cell number or thickness of the neuroepithelium structure within the cerebellar anlage at E12.5 (Figs. 2G, H). Lobulation of the cerebellum commences around E17.5 in mice, therefore, we analyzed the cerebellum of our mutants around this critical time point. At E15 and E18, the structure of the cerebellar anlage was similar in control and mutant embryos and in situ RNA hybridization analysis of neurogenic markers including Mash1, Math1 and NeuroD also failed to detect differences between the control and mutant animals (data not shown). In addition, few remaining Nestin-positive progenitor cells were detected in the ventricular zone of both mutant and control embryos (data not shown). Taken together, the analysis at E15 and E18 did not reveal alterations in the developing cerebellar anlage of mutant compared to control embryos.

Conditional ablation of the mNumb gene leads to a delay in granule cell precursor maturation

We have shown previously that Numb is expressed in the external germinal layer (EGL) and the internal granule cell layer (IGL) as well as in the Purkinje cell layer of the

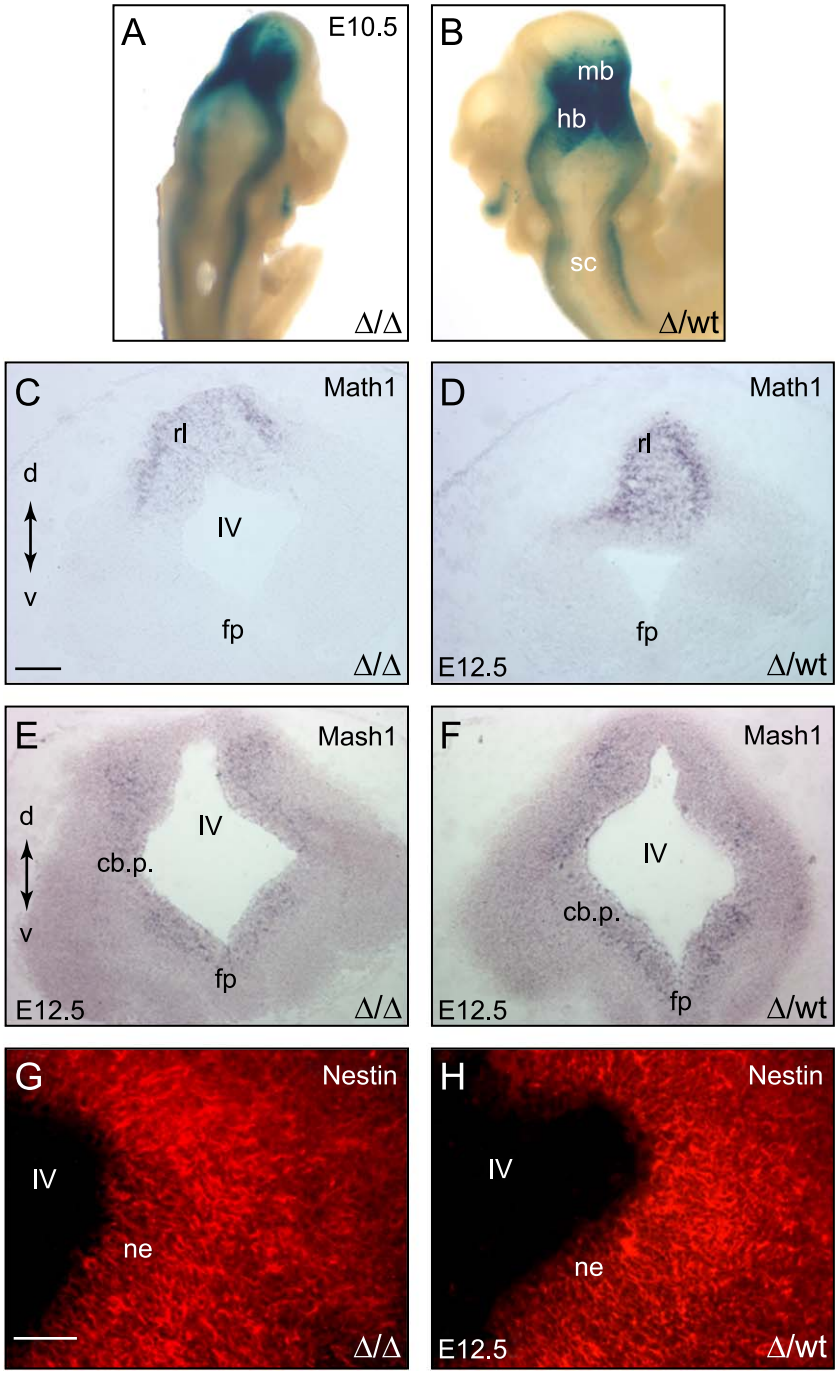

Fig. 2. Embryonic analysis of conditional *Numb*-deficient mice. (A) E10.5 homozygous floxed *Numb* (Δ/Δ) animals carrying an *En2-Cre* and *R26R* allele showed recombined cells (blue) in the midbrain–hindbrain region of the brain. (B) Heterozygous E10.5 floxed *Numb* (Δ/wt) animals carrying an *En2-Cre* and *R26R* allele revealed a similar restricted distribution of recombined cells (blue) in the midbrain–hindbrain region of the developing brain. (C–F) In situ RNA hybridization on cross-sections through the neural tube, dorsal to the top and ventral to the bottom, of E12.5 mutant animals (Δ/Δ) showed normal expression of Math1 (C) and Mash1 (E) mRNA in the cerebellar primordium compared to control littermates (D, F: Δ/wt). (G, H) Immunostaining with anti-Nestin antibodies showed a similar expression pattern at E12.5 in the cerebellar neuroepithelium of mutant animals (G: Δ/Δ) compared to control animals (H: Δ/wt) (in G and H, one half of the cerebellar primordium is depicted with dorsal to the top and ventral to the bottom). Scale bars: in C, 100 μm for C–F; in G, 50μm for G,H; cb.p.= cerebellar primordium, fp= floorplate, hb= hindbrain, mb= midbrain, ne= neuroepithelium, IV= fourth ventricle, sc= spinal cord.

cerebellum of young postnatal (P4) mice (Stump et al., 2002). Thus, we analyzed granule cell differentiation in our mutants in more detail at this time point by examining the expression of Math1 and NeuroD. Math1 is expressed predominantly in the outer portion of the EGL by mitotic progenitors and is downregulated by postmitotic granule cell precursors, while NeuroD is expressed in the inner aspects of the EGL and in the

developing IGL by postmitotic granule cells (Oberdick et al., 1998). Midsagittal sections revealed a reduction in the size of the mutant cerebellum at P4 (Fig. 3A) when both granule cell precursors and Purkinje cells start to undergo terminal maturation. Math1 RNA could be detected in the outer EGL (Figs. 3A, B) and NeuroD RNA in the inner

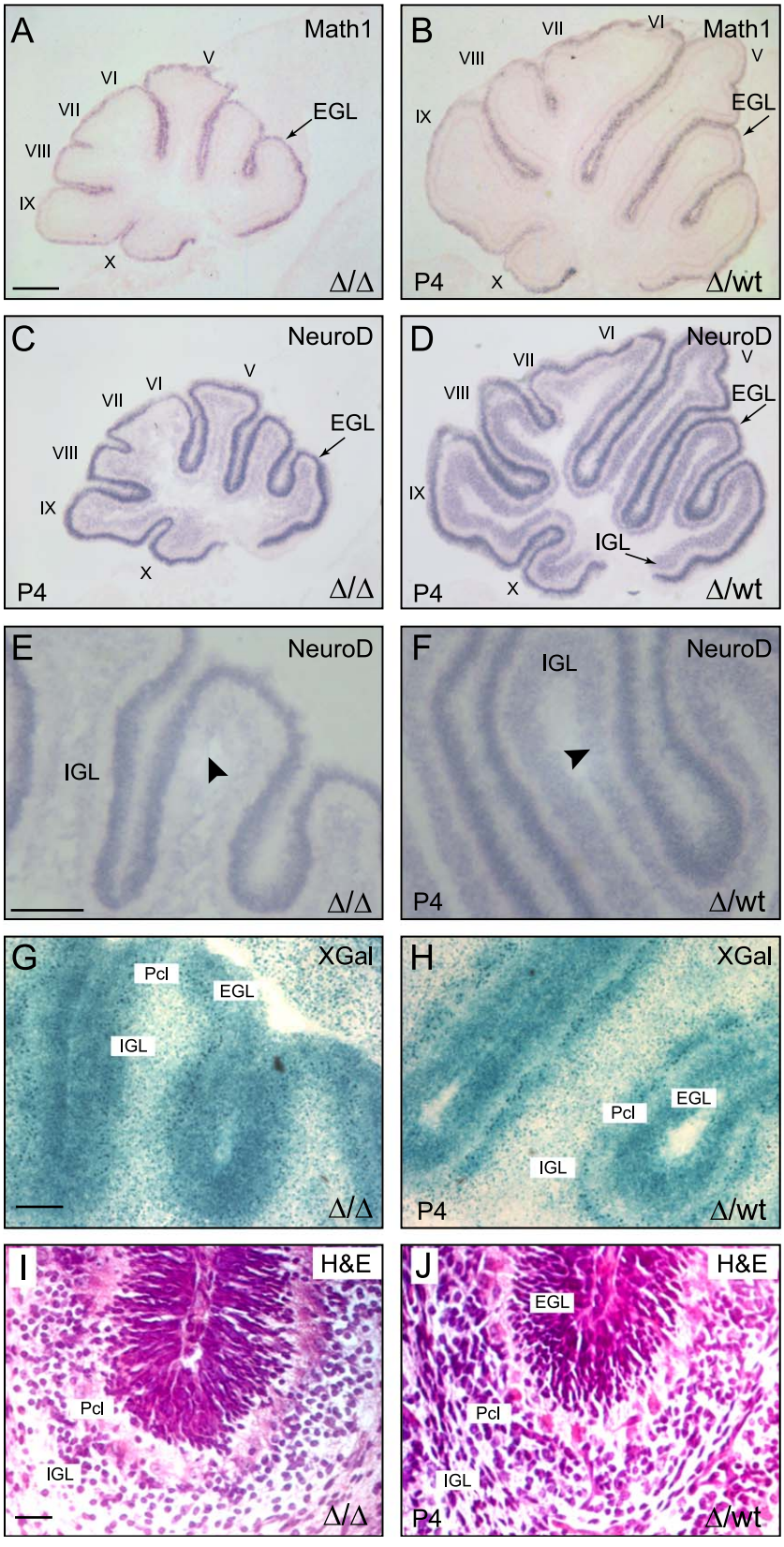

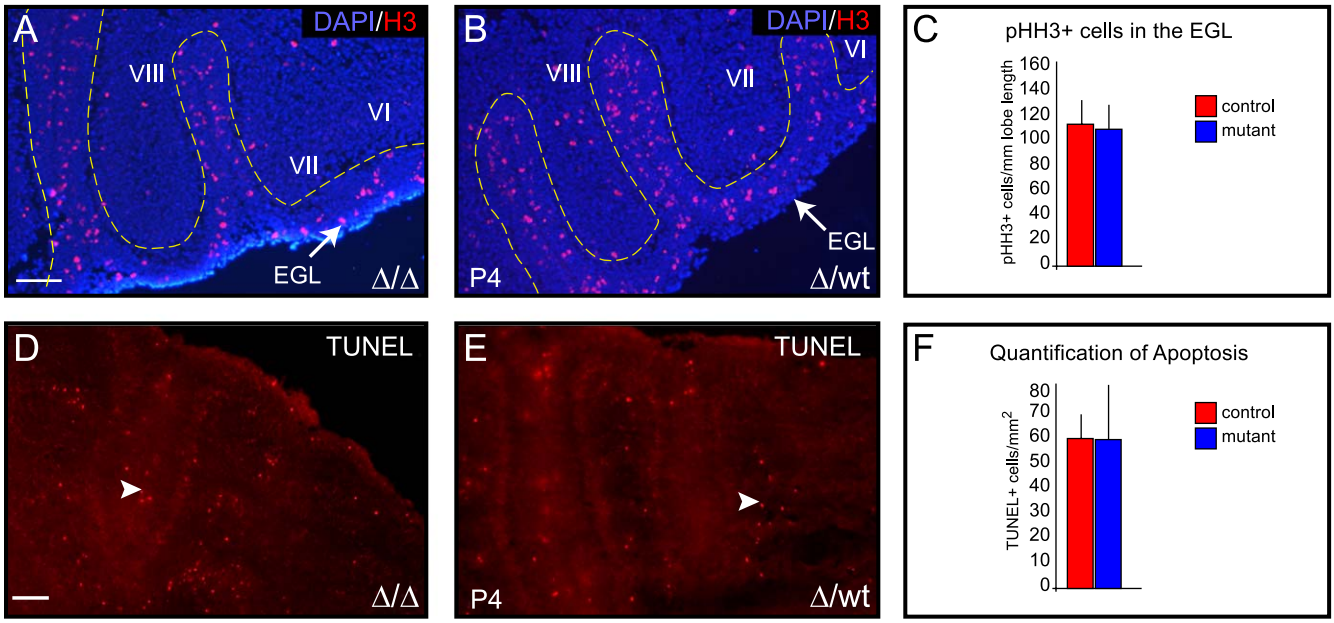

Fig. 4. Characterization of granule cell precursor proliferation and apoptosis in the early postnatal cerebellum. Immunostaining of P4 cerebellar sections (lobes VI, VII and VIII) with an anti-pH3 antibody to identify cells in the M-phase of the cell cycle revealed proliferating cells in the EGL (delineated by dotted line) of the mutant (A) and control (B) animals. Quantification using NIH Image software indicated that mutant and control animals have similar numbers of proliferating cells in the EGL per mm lobe length (C). TUNEL-staining (D, E) (white arrowhead) and quantification of apoptotic cells (F) per cerebellar area did not reveal differences in the apoptotic rate in the mutant when compared to the control animals at P4. (C, D, G: red bars = control; blue bars = mutant). Scale bars: in A and E, 100 μm for A, B, E, F.

EGL and IGL of both mutant and control littermates (Figs. 3C, D). However, NeuroD RNA levels were decreased in the IGL of mutant animals (Figs. 3E, F). Concomitant, histological staining revealed fewer cells in the IGL of mutant mice, suggesting that less granule cell precursors had migrated into the mutant cerebellum compared to the controls. Moreover, the EGL of the mutant cerebellum is more densely packed compared to the EGL of the control littermates (Figs. 3I, J). This suggests that terminal maturation and migration of granule cell precursors is delayed in the cerebellum of P4 mutant mice. To address whether the reduced cerebellar size was due to a loss of recombined cells in the mutant compared to littermates with one functional *Numb* allele, we performed X-gal staining. Mutant and control cerebella displayed a similar level of β-galactosidase activity at P4 indicating recombined cells in both groups of animals. *Numb*-deficient cells are able to give rise to neurons in vivo, confirming previous observations (Petersen et al., 2002; Zhong et al., 2000) (Figs. 3G, H). Furthermore, our data suggest a developmental delay, which may account for the reduced cerebellar size observed in the early postnatal mutant mice.

Conditional ablation of mNumb does not alter proliferation characteristics of granule cell precursors at P4

Granule cell precursors of the inner EGL leave the cell cycle and commence differentiation in the first 3 weeks of postnatal life in the mouse (Hatten and Heintz, 1995; reviewed in Hatten et al., 1997). To account for the small size of the mutant cerebellum, we examined the proliferation characteristics of granule cell precursors in the EGL of P4 mutant and control mice by immunostaining with anti-pH3 antibodies. Most of the proliferating cells were in the outer EGL (Figs. 4A, B). Quantification of the number of pH3-positive cells in the EGL revealed a similar number of proliferating cells per lobe length in the mutant animals (105.9 +/− 21.0 cells/mm lobe length, four animals analyzed) compared to controls (110.7 +/− 23.8 cells/mm lobe length, three animals analyzed) (Fig. 4C). Moreover, to determine the cause of the reduction in the mutant cerebellum, we examined cell death by TUNEL analysis (Figs. 4D, E). Quantification of TUNEL-positive cells in the mutant (three animals) and control (three animals) cerebella did not reveal detectable differences in the apoptotic rate (Fig. 4F).

Fig. 3. Early postnatal cerebellar development is affected by *Numb* ablation. In situ RNA hybridization failed to reveal differences in Math1 mRNA expression in the outer portion of the external germinal layer (EGL) of mutant (A) and control (B) mice. In situ RNA hybridization for NeuroD showed expression restricted to the inner portion of the EGL and in the developing internal granule cell layer (IGL) in both mutant (C) and control (D) animals. Higher magnification pictures revealed reduced NeuroD mRNA expression in the developing IGL of the mutant (E) compared to the control (F) animals (arrowheads). Recombined cells (blue) were detectable in the developing cerebellum of mutant (G) as well as control (H) animals. Hematoxylin/Eosin staining revealed fewer cell bodies in the IGL of mutant (I) when compared to the control (J). Scale bars: in A, 500 μm for A–D; in E, 200 μm for E and F; in G, 100 μm for G and H; in I, 20 μm for I and J; Pcl = Purkinje cell layer.

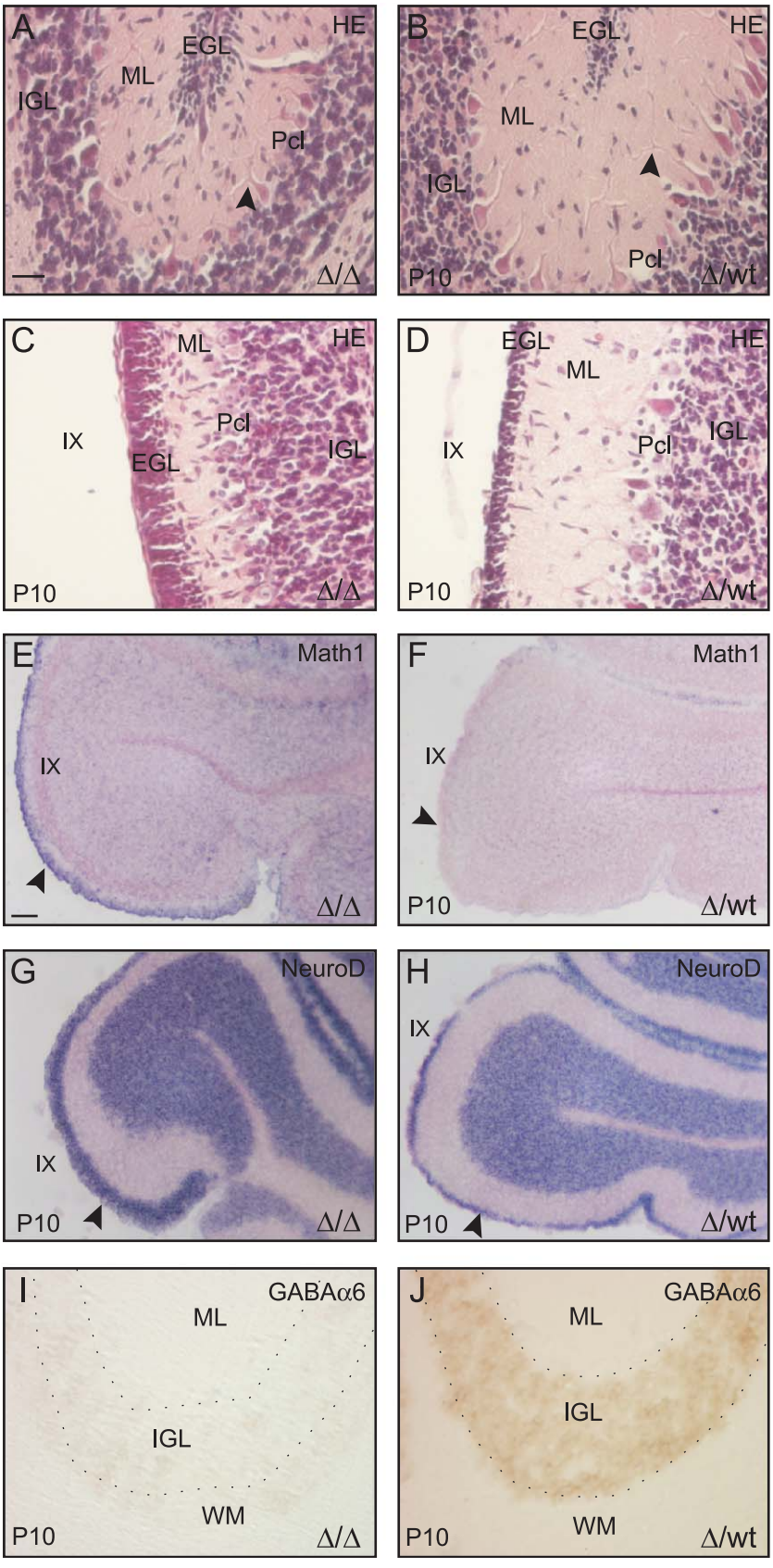
A
HE
EGL
ML
IGL
Pcl
Δ/Δ
B
EGL
HE
ML
IGL
Pcl
P10
Δ/wt
C
ML
HE
IX
Pcl
EGL
IGL
P10
Δ/Δ
D
EGL
ML
HE
IX
Pcl
IGL
P10
Δ/wt
E
Math1
IX
Δ/Δ
F
Math1
IX
P10
Δ/wt
G
NeuroD
IX
P10
Δ/Δ
H
NeuroD
IX
P10
Δ/wt
I
GABAα6
ML
IGL
WM
P10
Δ/Δ
J
GABAα6
ML
IGL
WM
P10
Δ/wt

Next, we addressed differentiation of the granule cells at later stages. At P10, histological staining revealed that the EGL of mutants is considerably thicker (Figs. 5A, C) than that of control animals (Figs. 5B, D). This is likely the result of an accumulation of granule cell precursors in the mutant EGL. In support of this interpretation, few Math1-expressing cells were detected in the outer EGL of control animals; however, the EGL of mutants still contained an appreciable number of Math1-positive cells (Figs. 5E, D arrowheads). Moreover, an increase in NeuroD-expressing cells was detected in the EGL of mutants compared to control animals (Figs. 5G, H arrowheads). Finally, GABAα6 receptor subunits, a marker of fully differentiated granule cells (Thompson and Stephenson, 1994), were clearly expressed in the IGL of control animals (Fig. 5J) while being hardly detectable in the IGL of mutant animals (Fig. 5I), thus, strengthening the hypothesis of a delay in terminal maturation of *Numb*-deficient granule cell precursors.

Conditional ablation of the mNumb gene leads to a delay in Purkinje cell maturation

Cerebellar Purkinje cell precursors cease proliferation around E13 in the mouse and migrate along the radial glial fibers to settle in a dense zone underlying the forming EGL. Terminal differentiation of Purkinje cells, however, occurs postnatally when they become arranged in a single cell layer and make contacts with the parallel fibers of the granule cells (Hatten and Heintz, 1995). To address the differentiation of Purkinje cells in the absence of Numb, we performed in situ hybridization with the Purkinje cell marker Calbindin D28k at P4 and P10 (Fig. 6). At P4, Calbindin D28k-expressing Purkinje cells were arranged into a multi-cell layer in both the mutant and control animals (Figs. 6A, B). However, at P10, while in the control animals, the Purkinje cells had formed a relatively homogeneous single cell layer, the Purkinje cells of the mutants were often seen in multiple layers, an indication of delayed development (Figs. 6C, D). As granule cells are partially responsible for the layered organization of the Purkinje cells, the reduced granule cell precursor development seen in the *Numb*-deficient animals may be partly responsible for the effects on the Purkinje cells. However, apart from the arrangement of Purkinje cell bodies into a single cell layer, Calbindin D28k immunostaining revealed a complex dendritic tree development in control animals, indicating fully mature Purkinje cells (Fig. 6F, white arrowhead) while the architecture of the dendritic tree in the mutants was less elaborate (Fig. 6E, white arrowhead). Confirming these data, histological staining illustrated reduced outgrowth of primary dendritic trees in the mutants (Fig. 5A, black arrowhead) in comparison to the elongated primary dendritic tree in the control animals (Fig. 5B, black arrowhead). It was also evident that the molecular layer (ML), formed predominantly by Purkinje cell dendritic trees, is narrowed in the mutant (Figs. 5A, C and 6E).

This reduced Purkinje cell development also explains the reduced size of the mutant cerebellum. Hence, these data indicate that terminal maturation of Purkinje cells in our mutants is affected and support the hypothesis of a delay in cerebellar development in *Numb*-deficient animals.

Conditional ablation of the mNumb gene leads to a reduction in adult cerebellar foliation and Purkinje cell number

Histological staining and morphological analysis revealed that ablation of the *mNumb* gene resulted in a reduced cerebellar foliation (Figs. 7A, B). To identify recombined cells in the brains of mutant and control animals, we stained sagittal hemisected adult brains with X-gal. Recombined, β-galactosidase-expressing cells were found in the molecular layer, granule cell layer and Purkinje cell layer of both control and mutant animals (Figs. 7F, G). The presence of recombined cells in the cerebellum of the conditionally *Numb*-ablated animals indicates that mNumb is not absolutely required for survival and differentiation of granule cells and Purkinje cells in vivo. To quantify the changes in cerebellar formation because of *Numb* ablation, we measured the lobe length along the Purkinje cell layer on consecutive 20 μm midline sagittal cerebellar sections of mutant and control animals (Figs. 7C, D). Some individual lobes of mutant cerebella were reduced in size (Fig. 7E) and lobes VI and VII were most severely affected (P value $<$ 0.001, Student's t test) in the mutants (5.9 +/− 0.02 mm) compared to control animals (7.47 +/− 0.25 mm). In addition, these lobes were often fused. Although the fusion was already apparent in the cerebellum of mutant animals at P4, the overall organization of the cell layers within the adult cerebellum was not affected (Figs. 7A, B).

We also performed Calbindin D28k in situ hybridization on sections of adult cerebellum to determine Purkinje cell number and distribution (Figs. 7C, D). In both adult control and mutant cerebella, Purkinje cells were arranged into a

Fig. 5. Development of granule cell precursors is affected by *Numb* ablation. Hematoxylin/Eosin staining showed an accumulation of granule cell precursors in the EGL of mutant (A, C) compared to the control P10 animals (B, D). Purkinje cells in the mutant (black arrowhead, A) have a shorter, less extensive dendritic tree compared to control animals (black arrowhead, B). In situ RNA hybridization showed maintained Math1 mRNA expression in the outer EGL of P10 mutant (E) compared to control animals (F). The arrowhead in E points to the outer EGL of the mutant animal and shows the increased Math1 mRNA expression compared to the control littermate (F; arrowhead). In situ RNA hybridization revealed an increase in cells expressing NeuroD in the EGL of mutant animals (G) compared to controls (H). Arrowheads in G and H point to the differences in NeuroD mRNA in the mutant (G) compared to the control animals (H). GABAα6 receptor subunit as a marker of mature granule cells is virtually absent in the mutants (I) while it is restricted to the IGL of the control animal (J). Scale bars: in A, 20 μm for A, B, C, D, I, J; in E, 100 μm for E, F, G, H; WM= white matter, ML= molecular layer, IGL= internal granule cell layer, Pcl= Purkinje cell layer.

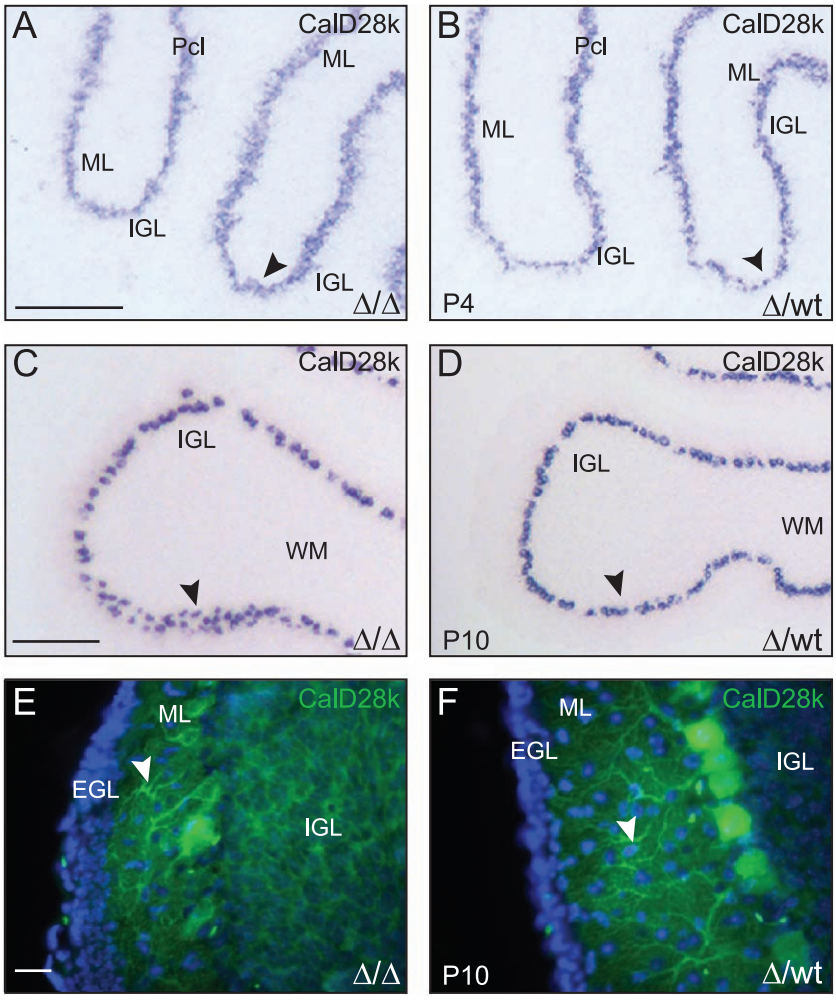

Fig. 6. Development of Purkinje cells is aberrant following *Numb* ablation. In situ RNA hybridization on sagittal sections of P4 cerebellum with a Calbindin D28k probe showed the arrangement of Purkinje cell bodies in a multi-cell layer in both mutant (A) and control (B) animals within a similar region between lobes V and VI. However, in the control animals (B) Purkinje cells had started to be arranged in a single cell layer, particularly at the base of the lobes, whereas in the mutants the PC remained in multiple layers (arrowheads A, B). Calbindin D28k in situ RNA hybridization at P10 revealed that Purkinje cells were arranged in a single cell layer (arrowhead in D) in the control (D) animals while they remained partially as a multi-cell layer (arrowhead in C) in the mutant (C). The images in C and D are of comparable regions of lobe IX in both the mutant and control animals. Purkinje cell dendritic trees (arrowheads) were less complex in the mutant (E) than in the control animals at P10 (F) as shown by Calbindin D28k immunostaining in lobe IX. The molecular layer is thicker in the control than in the mutant animals (E, F). Scale bars: in A, 200 μm for A, B; in C, 200 μm for C, D; in E, 20 μm for E, F.

single cell layer. However, Purkinje cell number was significantly reduced in the anterior lobes (control: 355 +/− 7; mutant: 310 +/− 23.5; P value < 0.001, Student's t test), in the central lobes (control: 235 +/− 1.1; mutant: 187 +/− 9.1; P value < 0.001, Student's t test) and in the posterior lobes (control: 212 +/− 47.4; mutant: 162 +/− 10.8; P value < 0.001, Student's t test) of the mutant, consistent with the observed reduction in lobe length (Fig. 7H). However, the calculated density of Purkinje cells remained unaltered in mutant animals (23.9 +/− 0.9 cells/mm)

Fig. 7. Morphological analysis of the adult cerebellum and quantification of the cerebellar size showing a reduction in adult cerebellar development. Hematoxylin staining of midline sagittal sections showed a marked reduction in the size of the mutant (A) cerebellum compared to control animals (B). Aberrant lobulation in the adult mutant cerebellum was also seen with fusion of lobes VI and VII (arrowheads in A, B). In situ RNA hybridization for Calbindin D28k on mutant (C) and control (D) cerebellar sections and quantification of lobe length revealed a reduction in the length of lobe 2/3, lobes 6/7 and lobe 10 in the mutant (**P < 0.01, Student's t test) (E). Owing to the fusion of lobes 6 and 7, they were measured together, from the posterior end of lobe 5 to the anterior end of lobe 8. Lineage tracing using the Cre-reporter transgene *R26R* showed that *Numb*-deficient, β-galactosidase expressing cells (blue) were present in all layers (molecular layer (ML), Purkinje cell layer (Pcl) and the internal granule cell layer (IGL)) of the adult mutant cerebellum (homozygous floxed *Numb En2-Cre* and *R26R*) (F) comparable to control animals (heterozygous floxed *Numb En2-Cre* and *R26R*) (G). Analysis of Purkinje cell number and density (H; see text) in adult animals revealed a significant (*P < 0.05, Student's t test) reduction in cell number within the anterior lobes (lobes 2–5) and the posterior lobes (lobes 9 and 10) and a highly significant (**P < 0.001, Student's t test) reduction in the Purkinje cell number within the central cerebellar lobes (lobes 6–8) of mutant animals (E, H: red bars = control; blue bars = mutant). Results shown are from a representative mutant animal and control littermate. Scale bars: in A, 1 mm for A, B; in C, 1mm for C, D.

compared to controls (25.5 +/ − 1.7 cells/mm). In addition, the granule cell layer of mutants showed a normal thickness and density of cells compared with control animals. Taking into account the overall reduction in size of the cerebellum, this suggests that the number of granule cells is also reduced in mutants.

In a few rare cases, we observed a strong phenotype in the mutant animals. In these mice, the size of the cerebellum was dramatically reduced and the vermis was virtually absent (Figs. 8A, B). The "typical" mutant (Fig. 8C) vermis is slightly flattened but clearly distinguishable from the lateral hemispheres, which appear normal. Histological

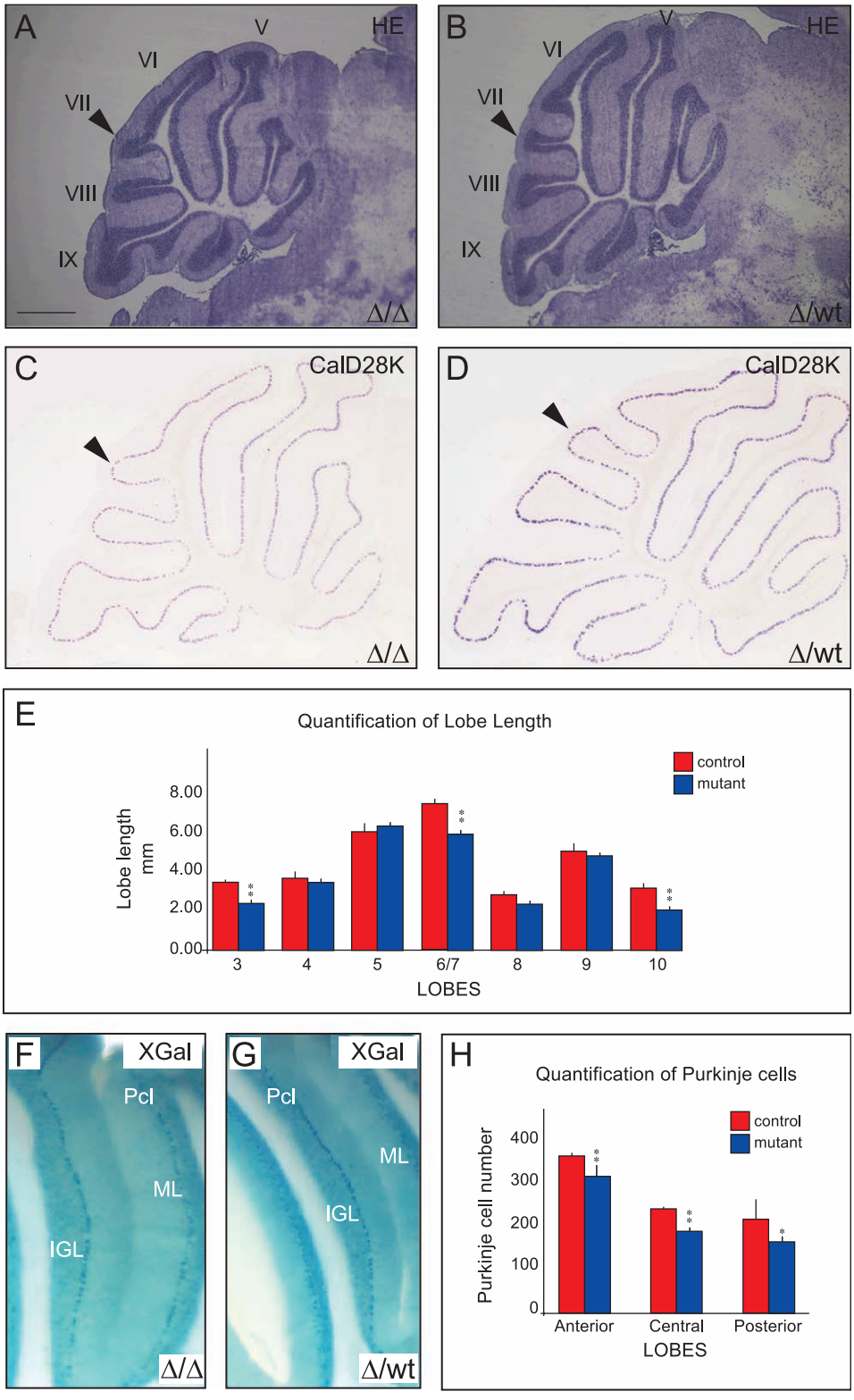

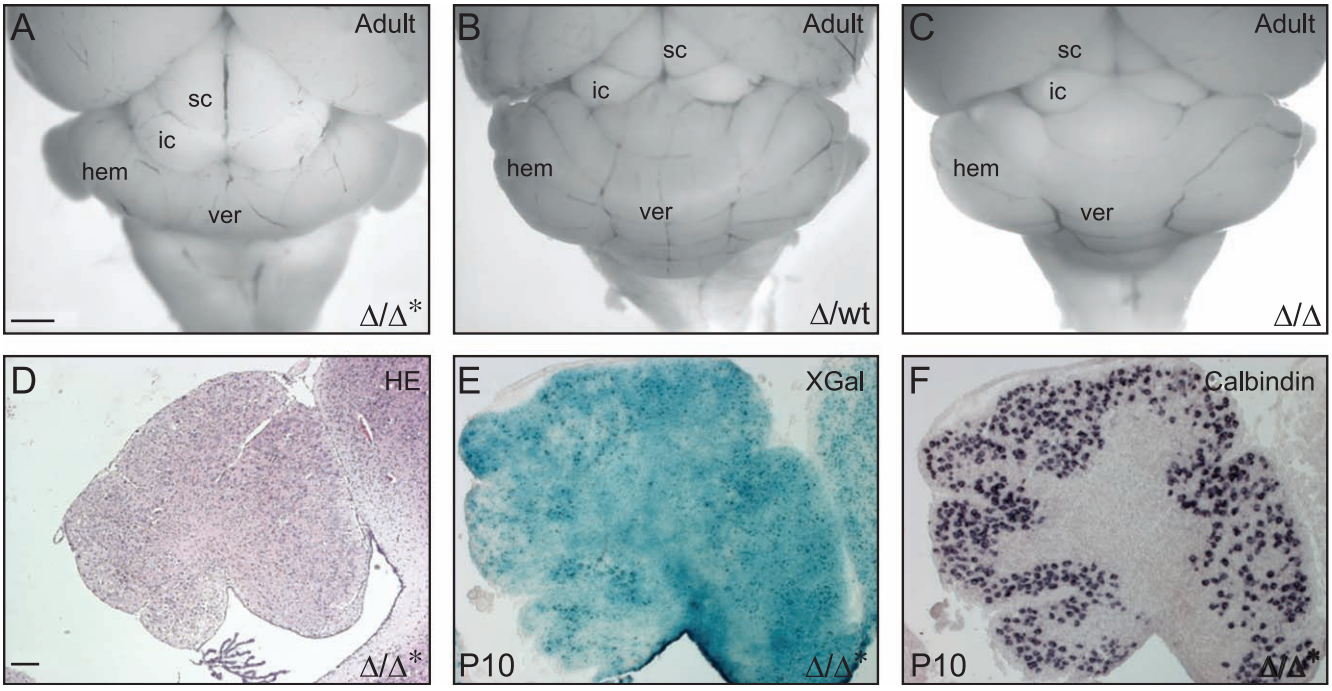

Fig. 8. Some mutant animals show a severe reduction in cerebellar formation and ataxic movements. Whole mount preparations of adult brains showed a lack of vermis (ver) and reduced lateral hemispheres (hem) in the severely affected mutant (Δ/Δ*) (A) animals compared to the control (Δ/wt) (B) and "typical" mutant (Δ/Δ) (C) animals. The midbrain colliculi were more exposed in these mutants than in the controls. Histological staining revealed that the layered cerebellar cortical structure is completely absent at P10 (D). In situ RNA hybridization for Calbindin D28k on midline sagittal sections of severely affected P10 mutant animals showed the totally aberrant foliation of the cerebellum due to the complete disorganization of Purkinje cells (F). X-Gal staining on a consecutive section demonstrated a marked reduction in cerebellar size and a virtually complete recombination in all cells of the cerebellum (E). Scale bars: in A, 1 mm for A, B, C; in D, 100 μm for D–F; ic= inferior colliculus, sc= superior colliculus.

staining of adult midsagittal sections of the "severe" mutant cerebellum revealed a severely aberrant lobulation (Fig. 8D). Calbindin D28k in situ hybridization of midsagittal sections at P10 revealed a complete disorganization of the Purkinje cells (Fig. 8F) and X-gal staining showed that virtually all the cells in the cerebellum of these "severe" mutants had undergone recombination (Fig. 8E). We also examined the granule cell marker NeuroD by in situ RNA hybridization and found no detectable expression in the "severe" mutants (data not shown). Behaviorally, these animals showed ataxia and died at 2–3 weeks of age. It remains to be determined whether this strong phenotype reflects variations in the recombination efficiency or genetic background effects.

Numb-deficient neuroepithelial cells generate reduced numbers of neurons in vitro

To gain more insight into the role of Numb in the regulation of cerebellar neurogenesis, we analyzed the

Fig. 9. Analysis of cell fate and differentiation of *Numb*-deficient progenitors in vitro. (A) Schematic representation of the experimental procedure. Cerebellar neuroepithelial cells were isolated from the midbrain–hindbrain region (indicated as β-galactosidase expressing cells (blue), excised region indicated by red quadrant) of E10.5 embryos. The cells were cultured for either 6.5 days (short-term culture) or 13 days (long-term culture) under defined conditions and subsequently fixed and stained with antibodies against β-galactosidase and, Nestin, β-TubulinIII, Calbindin D28k, O4 and SMA as well as Math1. (B) Western blot analysis performed on proteins isolated from cultured cerebellar neuroepithelial cells. Polyclonal anti-Numb antibodies recognized the 70 kDa Numb protein in cultures of control cells and revealed a major reduction in the amount of Numb protein in mutant cells. The residual amount of Numb protein detected in the mutant cell cultures is likely due to a number of unrecombined cells as β-galactosidase immunostaining revealed that approximately 85% of the plated cells underwent recombination. Anti-β-actin Western blot was performed to show equal loading of the proteins. Quantification and normalization of the Western blots to β-actin levels showed a 90% reduction in Numb protein in the mutant cell cultures. Nestin-positive progenitor cells (C), β-TubulinIII-positive granule cells (D), Calbindin D28k-positive Purkinje cells (E), SMA-positive smooth muscle cells (F), O4-positive oligodendrocytes (G) and Math1-positive granule cell precursors (H) were detected in both mutant and control cell cultures. (I) Quantification of marker expression by the recombined cells after 6.5 and 13 days in culture. Short-term culture revealed a highly significant (**$P < 0.01$, Student's t test) reduction in the generation of recombined *Numb*-deficient β-TubulinIII-positive granule cells, while the proportion of the other cell types was not significantly affected ($P > 0.05$, Student's t test) in the mutant compared to the control cell cultures. Long-term culture revealed a relative increase in the formation of recombined *Numb*-deficient β-TubulinIII-positive granule cells and suggested that additional granule cells are born between days 6.5 and 13 of the culture. After 13 days in vitro, there was no longer a significant difference between mutant and control cell populations. Insert: Quantification of Math1-positive cerebellar neuroepithelial cells after 6.5 and 13 days in culture. There was a significant increase in Math1-positive cells in mutant compared to control cultures in both short-term and long-term conditions ($P < 0.05$, Student's t test) (I: red bars= control; blue bars= mutant; n= number of embryos analyzed).

effects of *Numb* gene ablation on neuroepithelial cells in culture. Cerebellar neuroepithelial cells were isolated from E10.5 embryos. The cells were cultured under defined conditions, which allow the generation of cerebellar Purkinje cells, granule cells and glia (Stump and V. T.; unpublished observation) (Fig. 9A). By removing the neuro-

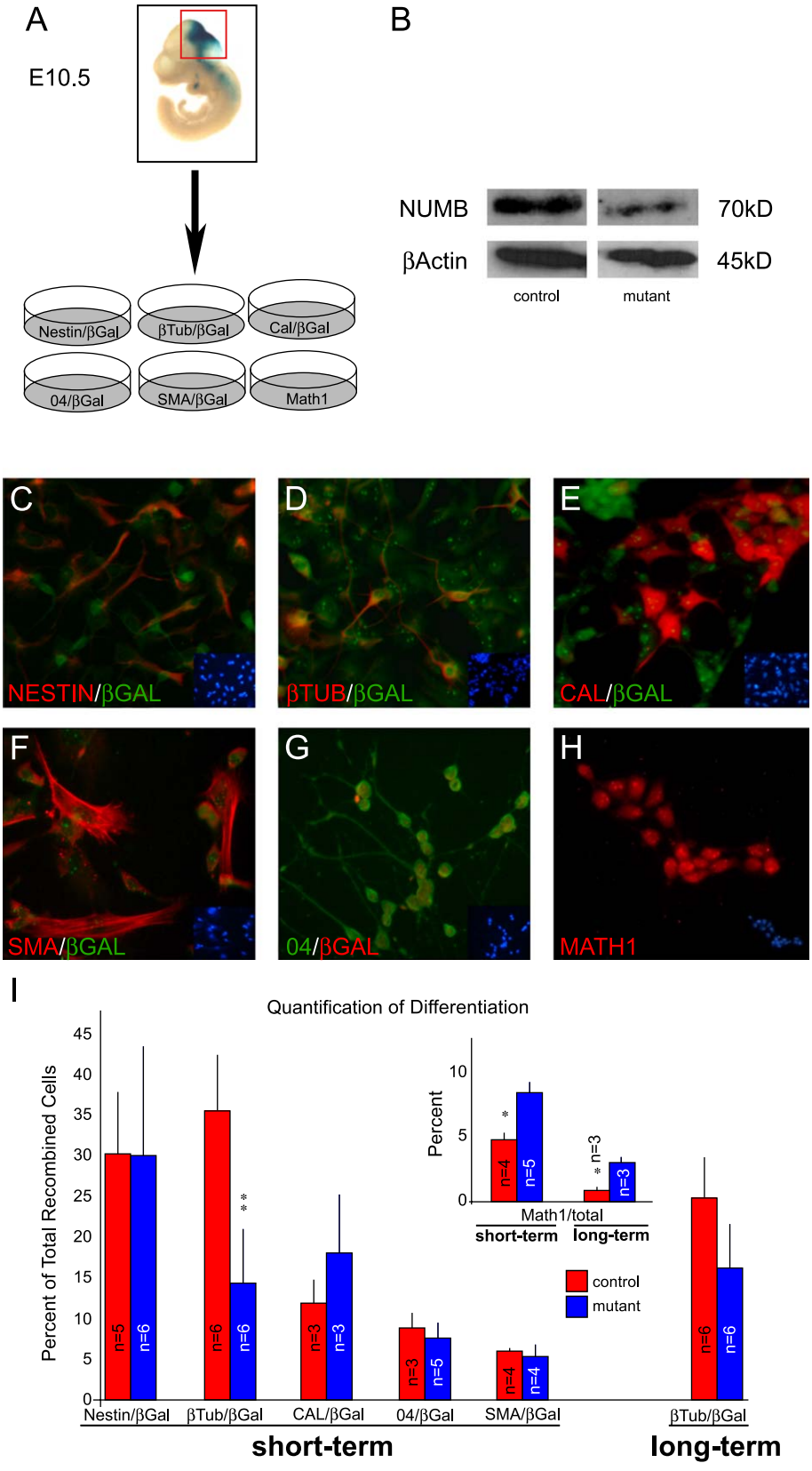

epithelial cells from their normal context, we wanted to characterize their cell fate choice and differentiation potential. Cells were isolated from homozygous floxed *Numb* animals and littermates with wild-type *Numb* alleles carrying the *En2-Cre* transgene and *R26R* reporter. After 6.5 days in vitro, β-galactosidase immunostaining revealed that 85% of the plated cells from both homozygous and control animals had undergone recombination. Western blot analysis performed on proteins isolated from sister cultures of neuroepithelial cells showed a 90% reduction in Numb protein levels in the mutant compared to control cells (Fig. 9B). The residual amount of Numb protein detected in the mutant cultures is likely due to the 15% of unrecombined cells. Next, we determined the percentages of recombined β-TubulinIII-positive granule cells, Calbindin D28k-positive Purkinje cells, Nestin-positive progenitor cells, O4-positive oligodendrocytes and smooth muscle actin (SMA)-positive smooth muscle-like cells by double-immunostaining with anti-β-galactosidase antibodies (Figs. 9C–H). Similar numbers of Nestin-positive progenitors were generated by both *Numb* mutant (30.3 +/− 13.4% of 1298 recombined cells counted) and control (30.5 +/− 7.9% of 910 recombined cells counted) cells (P value > 0.05; Student's t test) (Fig. 9I). Similarly, the number of Calbindin D28k-positive Purkinje cells (18.0 +/− 7.4% of 658 recombined cells counted) versus (11.9 +/− 3.2% of 953 recombined cells counted), O4-positive oligodendrocytes (5.3 +/− 1.4% of 694 recombined cells counted) versus (6.0 +/− 0.3% of 410 recombined cells counted) and smooth muscle actin (SMA)-positive smooth muscle cells (7.7 +/− 2.0% of 746 recombined cells counted) versus (8.8 +/− 2.0% of 973 recombined cells counted) was not significantly different (P value > 0.05; Student's t test) in cultures of mutant and control cells, respectively (Fig. 9I). By contrast, the number of β-TubulinIII-positive putative granule cells was significantly reduced (P value < 0.001; Student's t test) in the mutant (14.7 +/− 6.3% of 3686 recombined cells counted) compared to control (34.6 +/− 7.0% of 1397 recombined cells counted) (Fig. 9I). The average percentage of recombined cells was similar in cultures from control embryos (63.4 +/− 13.2%) and mutant embryos (62.7 +/− 9.4%) indicating similar plating, survival and proliferation rates.

Generation of granule cells from Numb-deficient progenitors in vitro is delayed

Combining the relative numbers of cells labeled, 92.7% of the cells in control cultures could be accounted for. However, 16.9% of recombined cells in the mutant cultures was not labeled by any of the differentiation markers analyzed. Since we did not observe an increase in Nestin, Calbindin D28k, GFAP, O4 and SMA-expressing cells in the cultures of mutant cells after 6.5 days in vitro, it is unlikely that the unaccounted for recombined cells underwent a switch in cell fate. In addition, death of this population can also be excluded, otherwise, a proportional increase in the other cell types would have been observed. Hence, to determine whether the recombined granule cells were delayed in their development or arrested in a precursor-like state, we cultured the cerebellar neuroepithelial cells for 13 days. We have observed previously that, under defined cell culture conditions, most of the granule cells are born within the first 24 h. However, the other cell types continue to be generated during the culture period (Stump and V. T., unpublished observation). In contrast to the 6.5 day cultures, the percentage of recombined granule cells generated in the mutant (16.4 +/− 5.5% of 1094 recombined cells counted) was no longer significantly different (P value > 0.05, Student's t test) to that observed in control cell cultures (25.0 +/− 5.2% of 1431 recombined cells counted) (Fig. 9I). The increase in granule cells in mutant cell cultures after 13 days suggests that additional *Numb*-deficient granule cells were generated between day 6.5 and day 13 in vitro compared to the control cultures. Hence, it is likely that *Numb*-deficient progenitors go through a transitory precursor-like state to generate granule cells and that this transition is delayed in the mutant cells. In support of this hypothesis, when we performed immunostaining with antibodies against Math1, a marker of mitotic granule cell precursors in the EGL, an increased number of Math1-positive granule cell precursors was found in short-term cultures of mutant cells (7.9 +/− 1.2% of 2876 cells counted) compared to control cells (4.9 +/− 0.9% of 2801 cells counted) in short-term culture (P value < 0.05, Student's t test) (Fig. 9I, insert). Although the number of Math1-positive cells declined after 13.5 days in culture, a significantly increased number of Math1-positive cells (P value < 0.05, Student's t test) was still present in the mutant (2.8 +/− 0.4% of 1282 cells counted) compared to control (1.5 +/− 0.4% of 1121 cells counted) (Fig. 9I, insert). Together, these data support the hypothesis that *Numb*-deficient progenitor cells are delayed in the progression and maturation to granule cells.

Discussion

In this report, we show that mNumb plays a role in regulating cerebellar granule cell differentiation, a function that is in agreement with the expression of mNumb in the EGL of the postnatal cerebellum. We also suggest that mNumb is involved in controlling the transition from a Nestin-negative neuroblast-like state to a terminally differentiated cerebellar granule cell. Additionally, we propose that mNumb is involved in terminal maturation of Purkinje cells.

We observed the first signs of delayed differentiation in the conditional Numb mutants in the early postnatal transition of proliferating EGL cells to postmitotic granule cells. Hence, early development of the cerebellum can proceed in the absence of mNumb. Furthermore, the expression of the proneural genes Mash1 and Math1 was not obviously affected in the conditional *mNumb* mutant mice indicating

that patterning and early cell fate decisions can occur in the absence of Numb. This may be due to a compensatory role of Numblike in early stages of cerebellar development. In situ RNA hybridization expression analysis confirmed that Numblike is expressed in the cerebellar neuroepithelium at E12.5 and overlaps with that of mNumb (data not shown). Hence, although the transition to a postmitotic granule cell is slowed in the absence of mNumb, Numblike may be able to functionally compensate for the mutation at all stages of cerebellar development. The delay, rather than a complete block of differentiation, may be the result of the time required for Numblike protein to accumulate in EGL cells. In the absence of reagents to unequivocally test this hypothesis, additional experiments will be required to substantiate this point further, including the regionalized inactivation of *mNumb* in the nervous system of *Numblike*-deficient animals. Targeting the ablation to a restricted portion of the neural tube should circumvent the early lethal effects observed in the *mNumb*, *Numblike*-double knockout animals (Petersen et al., 2002).

In contrast to the role of dNumb in cell fate decisions, mNumb does not seem to be involved in cell fate acquisition and patterning in the mouse central nervous system (Petersen et al., 2002). Taking advantage of the *R26R* reporter allele, we followed the fate of *mNumb*-ablated cells through adulthood. The presence of recombined cells in all layers of the cerebellar cortex of mutant animals and the fact that cells were arranged in layers with apparently normal cytoarchitecture indicate that mNumb is also not absolutely required for the generation of the terminally differentiated cerebellar cell types.

Recent data analyzing cortical neuroepithelial cells in culture indicate that mNumb can be asymmetrically localized in dividing cells (Shen et al., 2002). In E10 mouse neuroepithelial cells, asymmetric mNumb distribution does not correlate with cell fate acquisition. By contrast, in neural progenitors isolated during the peak neurogenic period (E13) mNumb shows a strong asymmetric localization in daughter cells and segregates to differentiating neurons while mNumb-lacking cells remain as progenitors (Shen et al., 2002). Hence, during early development of the nervous system, when cell divisions in the neural tube are thought to mainly expand the progenitor cell pool, mNumb may not directly affect cell fate choice. However, later in development, mNumb might be part of an intrinsic program that regulates cell differentiation (reviewed by Cayouette and Raff, 2002).

Our findings of a delayed granule cell development in the absence of mNumb may well reflect its role in regulating Notch signaling. Previous data suggest that Notch signaling is important for granule cell development (Solecki et al., 2001). Gain-of-function experiments activating Notch2 signaling in the EGL resulted in extended precursor proliferation and a block in granule cell differentiation (Solecki et al., 2001). Our data raise the possibility that mNumb regulates granule cell differentiation, potentially by modulating Notch2 signaling in mitotic EGL cells and enabling transition to a differentiated granule cell. However, we cannot exclude that Numb has other functions independent of Notch. In particular, the role of Numb as an adapter molecule with several binding partners and a putative link to growth factor signaling through the EH-domain indicates a potential for functions in other pathways (McGill et al., 2003; Nie et al., 2002; Yogosawa et al., 2003). Similarly, as described for BDNF −/− mice, *Numb*-deficient granule cell precursors accumulate in the EGL; however, in contrast to BDNF −/− cells, they fail to upregulate late differentiation markers in the EGL (Borghesani et al., 2002). Furthermore, Numb does not seem to act directly as a mitogenic cue but may regulate granule cells responsiveness to migration cues such as BDNF. Other factors involved in regulating proliferation and maturation of granule cells such as Sonic hedgehog (Wallace, 1999), CyclinD2 (Huard et al., 1999), Zic1 (Aruga et al., 1998), Gas1 (Liu et al., 2001), p27/Kip1 (Miyazawa et al., 2000) and NSCL-1 (Uittenbogaard et al., 1999) have been described previously.

We have previously shown that mNumb is also expressed by postnatal Purkinje cells (Stump et al., 2002). Our findings here indicate that Numb-deficient Purkinje cells display an aberrant dendritic morphology, with a reduced outgrowth of the primary dendritic tree. This result is in concordance with previous in vitro studies demonstrating that Notch signaling inhibits dendritic outgrowth but promotes dendritic branching in cortical neurons (Redmond et al., 2000) and suggests that mNumb is involved in promoting terminal maturation processes in Purkinje cells.

The layered structure of the EGL, with mitotic cells in the outer region progressing to the inner layers upon differentiation, is reminiscent of the delamination seen in the neuroepithelium, where Notch signaling regulates differentiation. Based on its widespread expression in neuroepithelial cells of the neural tube, mNumb is likely to be involved in the development of other CNS cell types and structures. Conditionally ablating *mNumb* from the neuroepithelium of *Numblike*-deficient mice resulted in an increased neuronal differentiation within the forebrain (Petersen et al., 2002). Although these data do not directly reflect our findings, the differences may be due to the multiple roles of Numb in nervous system development (Verdi et al., 1996), allelic differences between the two Numb mutants or genetic background of the experimental animals. Furthermore, different isoforms of Numb can have different effects ranging from blocking differentiation of progenitor cells to promoting neurogenesis, in vitro (Verdi et al., 1999) and in vivo (Dooley et al, 2003). Thus, spatial and temporal differences in the role of mNumb throughout the CNS development are likely and may require precise tuning. Based on the expression of the *En2-Cre* transgene in all cerebellar cell types in our mutants, the analysis of cell autonomous and cell non – autonomous functions of Numb will require lineage specific ablation.

In summary, we show that mNumb appears not to be involved in cell fate determination in the cerebellum but rather in promoting terminal differentiation. The task remains to integrate all signals and pathways with mNumb function in the formation of the cerebellum.

Acknowledgments

We would like to thank Dr. A. Joyner and Dr. P. Soriano for providing transgenic animals for this study. We thank Dr. Michel Aguet for providing the floxed *Numb* animals and for his continuous support. We thank Dr. W. Zhong for helpful comments and Drs. D. Junghans, R. Kirch and R. Cassada for critical reading of the manuscript. We are also grateful to Dr. J.P. Magyar for assistance with computer analysis of Purkinje cell numbers. The Rat-401 anti-Nestin antibody developed by Dr. S. Hockfield was obtained from the Developmental Studies Hybridoma Bank maintained by The University of Iowa, Department of Biological Sciences, Iowa City, IA 52242, under the contract NO1-HD-7-3263 from the NICHD. The Math1 antibody was a kind gift from Dr. J. Johnson. We thank Dr. M. Schwab for providing the O4 antibody and Dr. H. Okano for the Numb antibody. This work was supported by the Supported by the Swiss National Center of Competence in Research "Neural Plasticity and Repair" and the Deutsche Forschungsgemeinschaft (DFG).

References

Aruga, J., Minowa, O., Yaginuma, H., Kuno, J., Nagai, T., Noda, T., Mikoshiba, K., 1998. Mouse Zic1 is involved in cerebellar development. J. Neurosci. 18, 284–293.

Ben-Arie, N., Bellen, H.J., Armstrong, D.L., McCall, A.E., Gordadze, P.R., Guo, Q., Matzuk, M.M., Zoghbi, H.Y., 1997. Math1 is essential for genesis of cerebellar granule neurons. Nature 390, 169–172.

Borghesani, P.R., Peyrin, J.M., Klein, R., Rubin, J., Carter, A.R., Schwartz, P.M., Luster, A., Corfas, G., Segal, R.A., 2002. BDNF stimulates migration of cerebellar granule cells. Development 129, 1435–1442.

Cayouette, M., Raff, M., 2002. Asymmetric segregation of Numb: a mechanism for neural specification from *Drosophila* to mammals. Nat. Neurosci. 5, 1265–1269.

Chenn, A., McConnell, S.K., 1995. Cleavage orientation and the asymmetric inheritance of Notch1 immunoreactivity in mammalian neurogenesis. Cell 82, 631–641.

de la Pompa, J.L., Wakeham, A., Correia, K.M., Samper, E., Brown, S., Aguilera, R.J., Nakano, T., Honjo, T., Mak, T.W., Rossant, J., Conlon, R.A., 1997. Conservation of the Notch signalling pathway in mammalian neurogenesis. Development 124, 1139–1148.

Dho, S.E., Jacob, S., Wolting, C.D., French, M.B., Rohrschneider, L.R., McGlade, C.J., 1998. The mammalian numb phosphotyrosine-binding domain. Characterization of binding specificity and identification of a novel PDZ domain-containing numb binding protein, LNX. J. Biol. Chem. 273, 9179–9187.

Dooley, C.M., James, J., McGlade, J.C., Ahmad, I., 2003. Involvement of numb in vertebrate retinal development: evidence for multiple roles of numb in neural differentiation and maturation. J. Neurobiol. 54, 313–325.

Frise, E., Knoblich, J.A., Younger-Shepherd, S., Jan, L.Y., Jan, Y.N., 1996. The *Drosophila* Numb protein inhibits signaling of the Notch receptor during cell–cell interaction in sensory organ lineage. Proc. Natl. Acad. Sci. U. S. A. 93, 11925–11932.

Guillemot, F., Joyner, A.L., 1993. Dynamic expression of the murine Achaete-Scute homologue Mash-1 in the developing nervous system. Mech. Dev. 42, 171–185.

Guo, M., Jan, L.Y., Jan, Y.N., 1996. Control of daughter cell fates during asymmetric division: interaction of Numb and Notch. Neuron 17, 27–41.

Hatten, M.E., Heintz, N., 1995. Mechanisms of neural patterning and specification in the developing cerebellum. Annu. Rev. Neurosci. 18, 385–408.

Hatten, M.E., Alder, J., Zimmerman, K., Heintz, N., 1997. Genes involved in cerebellar cell specification and differentiation. Curr. Opin. Neurobiol. 7, 40–47.

Heitzler, P., Simpson, P., 1991. The choice of cell fate in the epidermis of *Drosophila*. Cell 64, 1083–1092.

Huard, J.M., Forster, C.C., Carter, M.L., Sicinski, P., Ross, M.E., 1999. Cerebellar histogenesis is disturbed in mice lacking cyclin D2. Development 126, 1927–1935.

Liu, Y., May, N.R., Fan, C.M., 2001. Growth arrest specific gene 1 is a positive growth regulator for the cerebellum. Dev. Biol. 236, 30–45.

Lundell, M.J., Lee, H.K., Perez, E., Chadwell, L., 2003. The regulation of apoptosis by Numb/Notch signaling in the serotonin lineage of *Drosophila*. Development 130, 4109–4121.

Lutolf, S., Radtke, F., Aguet, M., Suter, U., Taylor, V., 2002. Notch1 is required for neuronal and glial differentiation in the cerebellum. Development 129, 373–385.

Mayer, B.J., 1999. Endocytosis: EH domains lend a hand. Curr. Biol. 9, R70–R73.

Mayer-Proschel, M., Kalyani, A.J., Mujtaba, T., Rao, M.S., 1997. Isolation of lineage-restricted neuronal precursors from multipotent neuroepithelial stem cells. Neuron 19, 773–785.

McGill, M.A., McGlade, C.J., 2003. Mammalian numb proteins promote Notch1 receptor ubiquitination and degradation of the Notch1 intracellular domain. J. Biol. Chem. 278, 23196–23203.

Miyazawa, K., Himi, T., Garcia, V., Yamagishi, H., Sato, S., Ishizaki, Y., 2000. A role for p27/Kip1 in the control of cerebellar granule cell precursor proliferation. J. Neurosci. 20, 5756–5763.

Muskavitch, M.A., 1994. Delta-notch signaling and *Drosophila* cell fate choice. Dev. Biol. 166, 415–430.

Nie, J., McGill, M.A., Dermer, M., Dho, S.E., Wolting, C.D., McGlade, C.J., 2002. LNX functions as a RING type E3 ubiquitin ligase that targets the cell fate determinant Numb for ubiquitin-dependent degradation. EMBO J. 21, 93–102.

O'Connor-Giles, K.M., Skeath, J.B., 2003. Numb inhibits membrane localization of Sanpodo, a four-pass transmembrane protein, to promote asymmetric divisions in *Drosophila*. Dev. Cell 5, 231–243.

Oberdick, J., Baader, S.L., Schilling, K., 1998. From zebra stripes to postal zones: deciphering patterns of gene expression in the cerebellum. Trends Neurosci. 21, 383–390.

Petersen, P.H., Zou, K., Hwang, J.K., Jan, Y.N., Zhong, W., 2002. Progenitor cell maintenance requires numb and numblike during mouse neurogenesis. Nature 419, 929–934.

Rao, M.S., Mayer-Proschel, M., 1997. Glial-restricted precursors are derived from multipotent neuroepithelial stem cells. Dev. Biol. 188, 48–63.

Redmond, L., Oh, S.R., Hicks, C., Weinmaster, G., Ghosh, A., 2000. Nuclear Notch1 signaling and the regulation of dendritic development. Nat. Neurosci. 3, 30–40.

Rhyu, M.S., Jan, L.Y., Jan, Y.N., 1994. Asymmetric distribution of numb protein during division of the sensory organ precursor cell confers distinct fates to daughter cells. Cell 76, 477–491.

Salcini, A.E., Confalonieri, S., Doria, M., Santolini, E., Tassi, E., Minenkova, O., Cesareni, G., Pelicci, P.G., Di Fiore, P.P., 1997. Binding specificity and in vivo targets of the EH domain, a novel protein–protein interaction module. Genes Dev. 11, 2239–2249.

Shen, Q., Zhong, W., Jan, Y.N., Temple, S., 2002. Asymmetric Numb distribution is critical for asymmetric cell division of mouse cerebral cortical stem cells and neuroblasts. Development 129, 4843–4853.

Silva, A.O., Ercole, C.E., McLoon, S.C., 2002. Plane of cell cleavage and numb distribution during cell division relative to cell differentiation in the developing retina. J. Neurosci. 22, 7518–7525.

Solecki, D.J., Liu, X.L., Tomoda, T., Fang, Y., Hatten, M.E., 2001. Activated Notch2 signaling inhibits differentiation of cerebellar granule neuron precursors by maintaining proliferation. Neuron 31, 557–568.

Soriano, P., 1999. Generalized lacZ expression with the ROSA26 Cre reporter strain. Nat. Genet. 21, 70–71.

Spana, E.P., Doe, C.Q., 1996. Numb antagonizes Notch signaling to specify sibling neuron cell fates. Neuron 17, 21–26.

Stump, G., Durrer, A., Klein, A.L., Lutolf, S., Suter, U., Taylor, V., 2002. Notch1 and its ligands Delta-like and Jagged are expressed and active in distinct cell populations in the postnatal mouse brain. Mech. Dev. 114, 153–159.

Thompson, C.L., Stephenson, F.A., 1994. GABAA receptor subtypes expressed in the cerebellar granule cells: a developmental study. J. Neurochem. 62, 2037–2044.

Uittenbogaard, M., Peavy, D.R., Chiaramello, A., 1999. Expression of the bHLH gene NSCL-1 suggests a role in regulating cerebellar granule cell growth and differentiation. J. Neurosci. Res. 57, 770–781.

Verdi, J.M., Schmandt, R., Bashirullah, A., Jacob, S., Salvino, R., Craig, C.G., Program, A.E., Lipshitz, H.D., McGlade, C.J., 1996. Mammalian NUMB is an evolutionarily conserved signaling adapter protein that specifies cell fate. Curr. Biol. 6, 1134–1145.

Verdi, J.M., Bashirullah, A., Goldhawk, D.E., Kubu, C.J., Jamali, M., Meakin, S.O., Lipshitz, H.D., 1999. Distinct human NUMB isoforms regulate differentiation vs. proliferation in the neuronal lineage. Proc. Natl. Acad. Sci. U. S. A. 96, 10472–10476.

Wakamatsu, Y., Maynard, T.M., Jones, S.U., Weston, J.A., 1999. NUMB localizes in the basal cortex of mitotic avian neuroepithelial cells and modulates neuronal differentiation by binding to NOTCH-1. Neuron 23, 71–81.

Wallace, V.A., 1999. Purkinje-cell-derived sonic hedgehog regulates granule neuron precursor cell proliferation in the developing mouse cerebellum. Curr. Biol. 9, 445–448.

Wan, S., Cato, A.M., Skaer, H., 2000. Multiple signalling pathways establish cell fate and cell number in *Drosophila malpighian* tubules. Dev. Biol. 217, 153–165.

Wang, S., Younger-Shepherd, S., Jan, L.Y., Jan, Y.N., 1997. Only a subset of the binary cell fate decisions mediated by Numb/Notch signaling in *Drosophila* sensory organ lineage requires suppressor of hairless. Development 124, 4435–4446.

Yogosawa, S., Miyauchi, Y., Honda, R., Tanaka, H., Yasuda, H., 2003. Mammalian Numb is a target protein of Mdm2, ubiquitin ligase. Biochem. Biophys. Res. Commun. 302, 869–872.

Zhong, W., 2003. Diversifying neural cells through order of birth and asymmetry of division. Neuron 37, 11–14.

Zhong, W., Feder, J.N., Jiang, M.M., Jan, L.Y., Jan, Y.N., 1996. Asymmetric localization of a mammalian numb homolog during mouse cortical neurogenesis. Neuron 17, 43–53.

Zhong, W., Jiang, M.M., Weinmaster, G., Jan, L.Y., Jan, Y.N., 1997. Differential expression of mammalian Numb, Numblike and Notch1 suggests distinct roles during mouse cortical neurogenesis. Development 124, 1887–1897.

Zhong, W., Jiang, M.M., Schonemann, M.D., Meneses, J.J., Pedersen, R.A., Jan, L.Y., Jan, Y.N., 2000. Mouse numb is an essential gene involved in cortical neurogenesis. Proc. Natl. Acad. Sci. U. S. A. 97, 6844–6849.

Zilian, O., Saner, C., Hagedorn, L., Lee, H.Y., Sauberli, E., Suter, U., Sommer, L., Aguet, M., 2001. Multiple roles of mouse Numb in tuning developmental cell fates. Curr. Biol. 11, 494–501.

Zinyk, D.L., Mercer, E.H., Harris, E., Anderson, D.J., Joyner, A.L., 1998. Fate mapping of the mouse midbrain–hindbrain constriction using a site-specific recombination system. Curr. Biol. 8, 665–668.